Metabotropic Receptor-Activated Calcium Increases and Store-Operated Calcium Influx in Mouse Müller Cells

Noel Da Silva,[1,2] *Caroline E. Herron,*[3] *Kelly Stevens,*[2,4] *Christine A. B. Jollimore,*[1,4] *Steven Barnes,*[2,4] *and Melanie E. M. Kelly*[1,4]

Purpose. Metabotropic receptor agonists that signal through G_q-coupled pathways increase Ca^{2+} in mammalian Müller cells by release from intracellular stores and Ca^{2+} influx pathways that have not been well described. The authors examined the involvement of voltage-dependent and non–voltage-dependent Ca^{2+} channels in metabotropic muscarinic receptor-activated Ca^{2+} increases and store-operated Ca^{2+} influx in cultured mouse Müller cells.

Methods. Intracellular Ca^{2+} was measured using fluorescence imaging with the ratiometric dye fura-2. Currents were recorded using the whole-cell patch-clamp recording method. mRNA and protein were identified using reverse transcriptase polymerase chain reaction (RT-PCR) and immunocytochemical approaches.

Results. The muscarinic receptor agonist carbachol (3–20 μM) produced increases in Ca^{2+} that were blocked by the muscarinic receptor antagonists atropine and pirenzepine. RT-PCR confirmed mRNA for metabotropic M1 muscarinic receptors. Depletion of Ca^{2+} stores by the sarcoplasmic/endoplasmic Ca^{2+} ATPase (SERCA) inhibitors thapsigargin and cyclopiazonic acid or the inhibition of phospholipase C occluded the carbachol-activated increase in Ca^{2+}. Carbachol-activated Ca^{2+} increases in Müller cells were enhanced by the diacylglycerol derivative 1-oleyl-2-acetyl-sn-glycerol and were blocked by transient receptor potential (TRP) channel blockers Gd^{3+}, La^{3+}, 2-APB, and flufenamic acid. Both muscarinic receptor activation and thapsigargin treatment depleted Ca^{2+} stores and produced Ca^{2+} entry that was attenuated by La^{3+}, 2-APB, Gd^{3+}, and flufenamic acid. mRNA and protein for TRPC1 and TRPC6 were present in mouse Müller cells, and carbachol activated a Gd^{3+}-sensitive, TRP-like cation channel.

Conclusions. Metabotropic muscarinic receptor-activated Ca^{2+} increases in mouse Müller cells require the release of Ca^{2+} from intracellular stores and the activation of Ca^{2+} entry that involves TRP-like cation channels but is independent of voltage-dependent Ca^{2+} channels. (*Invest Ophthalmol Vis Sci.* 2008;49:3065–3073) DOI:10.1167/iovs.07-1118

From the Departments of [1]Pharmacology, [2]Physiology & Biophysics, and [4]Ophthalmology, Dalhousie University, Halifax, Nova Scotia, Canada; and the [3]School of Biomolecular and Biomedical Sciences, Conway Institute, University College Dublin, Dublin, Ireland.

Supported by the National Science and Engineering Research Council (MEMK), Reynolds Fellowship in Pharmacology (NDS), and Piccione Visiting Professorship (CEH).

Submitted for publication August 27, 2007; revised January 21 and February 10, 2008; accepted April 28, 2008.

Disclosure: **N. Da Silva**, None; **C.E. Herron**, None; **K. Stevens**, None; **C.A.B. Jollimore**, None; **S. Barnes**, None; **M.E.M. Kelly**, None

The publication costs of this article were defrayed in part by page charge payment. This article must therefore be marked "*advertisement*" in accordance with 18 U.S.C. §1734 solely to indicate this fact.

Corresponding author: Melanie E. M. Kelly, Department of Pharmacology, Dalhousie University, 5859 University Avenue, Halifax, Nova Scotia, Canada B3H 4H7; melanie.kelly@dal.ca.

In glial cells, increases in cytosolic Ca^{2+} in response to exogenous stimuli contribute to glial intracellular and intercellular signaling and form the basis of glial Ca^{2+} excitability.[1,2] One well-established pathway for increasing Ca^{2+} in glial cells results from the activation of metabotropic receptors.[3] These receptors are commonly coupled to the $G_{q/11}$ activation of phospholipase C (PLC), leading to the hydrolysis of phosphatidyl inositol-4,5-bisphosphate (PIP_2) and the generation of diacylglycerol (DAG) and inositol trisphosphate (IP_3), which acts on IP_3 receptors (IP_3R) on endoplasmic reticulum (ER) Ca^{2+} stores.[4] Ca^{2+} release from the ER gives rise to Ca^{2+} influx through plasma membrane Ca^{2+} channels.[5–7] Several different classes of Ca^{2+}-permeable channels have been identified in glial cells—voltage-dependent Ca^{2+} channels and non–voltage-gated Ca^{2+} channels—including receptor-activated or store-operated channels (SOCs). In contrast to voltage-dependent Ca^{2+} channels, which activate with membrane depolarization, the activation of SOCs requires the depletion of internal Ca^{2+} stores.[6,7] Although the molecular identity of SOCs has not yet been well established, several members of the cation-permeable transient receptor potential canonical (TRPC) channel family may be candidate SOCs and may contribute to receptor- and store-operated capacitative Ca^{2+} entry in a variety of cells,[8–10] including glia.[11,12] Ca^{2+} entry may also occur through store-independent, noncapacitative routes that are frequently linked to DAG generation.[13–16]

Müller cells are radial glia that extend throughout the retina with apical processes projecting into the photoreceptor layer and endfeet forming the vitreal border of the inner retina. These cells regulate the extracellular milieu surrounding retinal neurons by the uptake of neurotransmitters and the regulation of extracellular ion levels.[17,18] A variety of applied stimuli, such as light and neurotransmitters, as well as mechanical and electrical stimuli increase Müller cell Ca^{2+} in isolated retinal preparations.[1] These evoked Ca^{2+} increases spread locally between coupled Müller cells as "calcium waves" and depend, in part, on the release of Ca^{2+} from IP_3-sensitive intracellular Ca^{2+} stores. It has been suggested that Ca^{2+} signaling in glial networks contributes to synaptic activity by allowing glial cells to respond to neuronal activity with the release of glial factors that modulate glial and neuronal activity.[2]

A number of metabotropic receptor agonists increase mammalian Müller cell Ca^{2+}. The most well established of these is adenosine triphosphate (ATP).[1,17] ATP activates metabotropic P2Y receptors in Müller cells to induce transient increases in Ca^{2+} by the release of Ca^{2+} from IP_3-sensitive intracellular stores, leading to the activation of Ca^{2+}-activated channels and Ca^{2+} influx.[1,19,20] In addition to ATP, muscarinic receptor agonists are able to generate increases in Ca^{2+} in Müller cells.[21] However, compared with ATP, relatively less is known about the signaling pathways coupled to muscarinic receptors in Müller cells. The aims of the present study were to characterize the pharmacologic and electrophysiologic properties of muscarinic receptor-activated Ca^{2+} influx in mouse Müller cells. Our experiments demonstrate that the activation of an M1 metabotropic receptor-coupled pathway in mouse Müller cells requires store-operated Ca^{2+} release and leads to the activation

of Ca^{2+} influx that is independent of voltage-gated Ca^{2+} channels but that involves Ca^{2+} entry through SOCs. We suggest that TRP channels of the TRPC family are candidate ion channels that may contribute to muscarinic receptor-activated Ca^{2+} increases in Müller cells and that pharmacologic block of these channels reduces receptor- and store-mediated Ca^{2+} influx.

Materials and Methods

Cell Culture Preparation

All cell culture reagents were from Sigma-Aldrich (Oakville, ON, Canada) unless noted otherwise. Mouse retinal Müller cell cultures were prepared as described previously,[22] with slight modifications. Seven- to 10-day-old C57B1/BJ mice were killed by decapitation in accordance with the ARVO Statement for the Use of Animals in Ophthalmic and Vision Research and the Dalhousie University Committee for the Use of Laboratory Animals. Eyes were enucleated, washed in Hanks balanced salt solution (HBSS) containing antibiotic mixture (penicillin 100 U/mL, streptomycin 100 μg/mL, amphotericin 25 μg/mL), and incubated at 37°C in HBSS containing antibiotic mixture for 1 hour in the dark to facilitate the subsequent separation of retinal tissue. Retinas were then removed from bisected eyeballs with care to avoid contamination with retinal pigment epithelium. Isolated retinas were rinsed three times in HBSS containing antibiotic mixture and dissociated by gentle mechanical trituration using a flame-polished sterile Pasteur pipette. The resultant cell aggregates were centrifuged for 5 minutes at 1000 rpm, and the supernatant was removed. The cell pellet was then resuspended in Dulbecco modified Eagle medium (DMEM) with 5.5 mM glucose, antibiotic mixture, and 10% fetal bovine serum, seeded into six-well tissue culture plates (VWR, Mississauga, ON, Canada), and placed in a CO_2 incubator at 37°C. The culture medium was left unchanged for 4 days and was replenished thereafter with vigorous washing to remove nonadherent cells. The medium was subsequently replaced every 3 days, and Müller cells, identified by their characteristic bipolar morphology, were isolated on cultures dishes and allowed to propagate. Purified Müller cell cultures were passaged biweekly at a ratio of 1:3 and were further identified by immunocytochemistry. For Ca^{2+} imaging, cells were plated at a density of 3×10^5 cells/mL in 35-mm glass-bottom culture dishes (Warner, Hamden, CT). For immunocytochemical staining or electrophysiology recording, cells were plated at a density of 10^5 cells/mL on glass coverslips (Fisher Scientific, Ottawa, ON, Canada).

Immunocytochemistry

Cells were rinsed once in PBS and fixed for 5 minutes at −20°C in 100% MeOH. After three washes of 10 minutes each in PBS, cells were incubated for 20 minutes in 0.3% Triton-X (Sigma-Aldrich). Nonspecific binding sites were blocked for one hour in 10% goat serum in PBS before incubation for 24 hours at 4°C with the primary antibodies anti–cellular retinaldehyde binding protein (CRALBP, 1:100; Abcam, Cambridge, MA), anti–glial fibrillary acidic protein (GFAP, 1:200; DAKO, Mississauga, ON, Canada), and anti-TRPC1 and -TRPC6 (TRPC1, TRPC6, 1:200; Alomone, Jerusalem, Israel). Antibody preabsorption controls were carried out using a 10:1 preabsorption of the peptide antigen with the primary antibody. Cells were then washed three times for 10 minutes each in PBS, followed by incubation for 2 hours at room temperature in secondary antibodies goat anti-mouse (Alexa Fluor 488, 1:400; Jackson ImmunoResearch, West Grove, PA) and goat anti-rabbit (CY3, 1:400; Jackson ImmunoResearch). After this, cells were washed twice for 10 minutes each in PBS and incubated (TO-PRO 3, 1:1000; Invitrogen, Burlington, ON, Canada) for 15 minutes to label the nuclei, followed by three 10-minute washes in PBS. Coverslips were mounted on slides (Vectashield; Vector Laboratories, Burlingame, CA), sealed with nail polish, and visualized on a laser scanning confocal microscope (510 Meta; Carl Zeiss Inc., Thornwood, NY).

RT-PCR

Total RNA from mouse Müller cells was isolated using a reagent (Trizol; Invitrogen) extraction procedure according to the manufacturer's instructions. After DNA digestion with RQ1 RNase-free DNase (Fisher Scientific, Nepean, ON, Canada), total RNA was reverse transcribed using Moloney murine leukemia virus (MMLV) reverse transcriptase (Fisher Scientific) and oligo(dt)12–18 primers specific for TPC1–7 channels (Table 1). cDNA amplification conditions for TRPC channels included 1-minute denaturation at 94°C, 35 cycles of 30 seconds at 94°C, 1-minute annealing at 52°C, 1-minute extension at 72°C, and final elongation of 10 minutes at 72°C. PCR primers for murine muscarinic receptors M1 to M5 were based on published sequences.[23] cDNA amplification for muscarinic receptors included 1-minute denaturation at 94°C, 40 cycles of 30 seconds at 94°C, 1-minute annealing at 60.1°C for M1 and M5, 67.2°C for M2, 57.2°C for M3, 66.2°C for M4, 1-minute extension at 72°C, and final elongation of 10 minutes at 72°C. PCR-amplified products were subjected to electrophoresis on a 1.5% agarose gel, stained with ethidium bromide, and visualized under ultraviolet light (Edas 290 and 1D software; Kodak, Toronto, ON, Canada). All reactions were replicated three or more times, and control reactions were performed with no cDNA template (data not shown). Confirmation of PCR amplification product sequences was carried out by restriction enzyme digest after DNA purification with a PCR purification kit (QIAminiElute; Qiagen, Mississauga, ON, Canada), or DNA fragments were isolated from the gel using a gel extraction kit (QIAquick; Qiagen) and sequenced using a commercial sequencing facility (DalGEN Microbial Genomics Centre, Dalhousie University). Product sequences matched the published sequences from GenBank (see Table 1 for accession numbers).

Table 1. Sequences of Mouse TRPC Primers Used for RT-PCR Reactions

Target	Fragment	Primer Sequence	Position in GenBank (accession no.)	Expected Size (bp)
mTRPC1	Sense	5′-ATGCTGTTGGCTGTGAATGC-3′	1085–1104 (NM011643)	427
	Antisense	5′-AGGAACTGCTGGCAATTTGAC-3′	1491–1511 (NM011643)	
mTRPC2	Sense	5′-AGACAAAGACAGCACCGAC-3′	637–655 (NM011644)	403
	Antisense	5′-CCTCAGACTCTTCCACATTC-3′	1020–1039 (NM011644)	
mTRPC3	Sense	5′-TTCATGTTCGGTGCTCGTG-3′	43–61 (NM019510)	831
	Antisense	5′-TTTGTGCCCGTGTCTTTC-3′	856–873 (NM019510)	
mTRPC4	Sense	5′-TCTGCAGATATCTCTGGGAAGGATGC-3′	1698–1723 (NM016984)	414
	Antisense	5′-AAGCTTTGTTCGAGCAAATTTCCATTC-3′	2112–2086 (NM016984)	
mTRPC5	Sense	5′-TGATACCAATGACGGCAGTG-3′	2748–2767 (NM009428)	287
	Antisense	5′-TACAATGCTGCTGTGCGATG-3′	3015–3034 (NM009428)	
mTRPC6	Sense	5′-GAAGTCACGAAGACCTTTC-3′	2728–2746 (NM013838)	332
	Antisense	5′-TGGCTCTAACGACAGTCTC-3′	3041–3059 (NM013838)	
mTRPC7	Sense	5′-ACCTGACAGCCAATAGCAC-3′	2394–2412 (NM012035)	240
	Antisense	5′-TCCCAAACTTCTCGCTGAG-3′	2615–2633 (NM012035)	

Calcium Imaging

Cells were briefly washed in Krebs-Ringer buffer (KRB) containing 125 mM NaCl, 5 mM KCl, 1 mM $CaCl_2$, 1 mM $MgCl_2$, 5.5 mM glucose, 20 mM HEPES, and 1 mM Na_2HPO_4, pH 7.4, before loading for 90 minutes at room temperature under continuous gentle agitation with 5 μM fura-2 AM (Invitrogen) and 0.1% pluronic acid. Ca^{2+}-free solutions were prepared by omitting Ca^{2+} from KRB and including 100 μM EGTA. Cells were transferred to a microscope chamber, washed for 30 minutes in KRB, and superfused at a rate of 1 mL/min. Cells were imaged with a cooled charge-coupled device camera (Photometrics SenSys; Roper Scientific, Tucson, AZ) fitted to a fluorescence microscope (UM-2; Nikon, Tokyo, Japan) using a 40× water immersion objective. To limit photodamage, ratio measurements were performed every 60 seconds during washing and every 2 seconds on drug application. Fura-2 fluorescence was produced by excitation from a 100-W xenon arc lamp with appropriate filter sets (excitation 340/380 nm; emission 510 nm; Sutter Instruments, Novato, CA). Müller cell fluorescence at 340 and 380 nm excitation was converted to ratiometric (340 nm/380 nm) values by an imaging system (Imaging Workbench 5.1; Indec BioSystems, Santa Clara, CA) and saved to the hard drive of a computer. The mean fura-2 ratio for each Müller cell was calculated over a large area (>90%) of the Müller cell, encompassing the cell body.

Patch-Clamp Recordings

Membrane currents were recorded from Müller cells using patch pipettes drawn from thin-walled borosilicate capillary tubes (ID, 1.1–1.2 mm; wall, 0.2 mm; MicroHematocrit; Drummond Scientific Co., Broomall, PA) with resistances ranging from 5 to 10 MΩ and containing 63 mM Cs-aspartate, 63 mM CsCl, 0.4 $CaCl_2$, 10 mM HEPES, 1 mM EGTA, 1 mM ATP, and 0.1 mM GTP at pH 7.2 (adjusted with CsOH). Free internal Ca^{2+} was estimated to be 60 nM (http://www.stanford.edu/%7ecpatton/webmaxc/webmaxclite115.htm). Current recordings were filtered at 1 kHz, acquired using a patch-clamp amplifier (Axopatch 1D; Molecular Devices Corp., Sunnyvale, CA), and digitized with an interface computer running BASIC-FASTLAB acquisition software (Indec BioSystems, Santa Clara, CA). All drugs were prepared before use in extracellular solution containing 65 mM Na-aspartate, 65 mM NaCl, 3 mM KCl, 2 mM $CaCl_2$, 1 mM $MgCl_2$, 11 mM glucose, 10 mM HEPES, 5 mM $NaHCO_3$, pH 7.2 (adjusted with NaOH). Liquid junction potentials were approximately 1 to 2 mV and were not corrected. Recordings were carried out at room temperature (21°C–23°C), and solutions and drugs were perfused at 1 mL/min.

Data Analysis

For imaging data, graphs represent ratiometric values (340 nm/380 nm) averaged from multiple cells (n = 3–26) imaged simultaneously in the field of view. Bar graphs represent normalized mean (± SEM) ratiometric data minus background values. For patch-clamp data, the current was normalized to cell capacitance. CCH-activated current represents current measured in the presence of CCH minus control current in the absence of CCH. Statistical comparisons were carried out using Sigma Plot 7.0 (Systat Software, Inc, San Jose, CA) or InStat (GraphPad, San Diego, CA) software, where differences between two groups were evaluated with Student's unpaired t-test and differences between more than two groups were analyzed using one-way ANOVA with post hoc Dunnett.

Drugs

U-73122 and CCH were obtained from Calbiochem (San Diego, CA). All other drugs were purchased from Sigma-Aldrich, unless otherwise specified in the text. Drugs were dissolved in water or dimethyl sulfoxide (DMSO) to make stock solutions of 1 to 100 mM and then were diluted to the final concentrations required using KRB or extracellular solution. Final DMSO concentrations were 0.1% or less.

Results

Müller Cell Culture

To examine the cell signaling pathways contributing to muscarinic receptor-activated Ca^{2+} increases in Müller cells, we established a purified mouse Müller cell culture (see Materials and Methods). The mammalian retina contains two different kinds of macroglia, retinal astrocytes, which are found at the nerve fiber layer of the inner retina, and Müller cells, which extend throughout the retina from the outer photoreceptor layer to the inner ganglion cell layer and are the principal retinal macroglia.[17,18] Müller cells were distinguished in culture by their characteristic bipolar morphology and positive staining for CRALBP (Fig. 1A) and GFAP (Fig. 1B). Figure 1C shows an overlay of CRALBP and GFAP staining in the Müller cell cytoplasm, with cell nuclei labeled with the nuclear dye TO-PRO 3.

CCH-Activated Ca^{2+} Increases: Muscarinic Activation of PLC and Ca^{2+} Stores Release

Figure 2A shows that short (30-second) applications of 20 μM CCH were able to repeatedly evoke transient increases in Ca^{2+} (measured by an increase in fura-2 ratio) in Müller cells that were blocked by the muscarinic receptor antagonist atropine (5 μM) and that were recovered on washout of the blocker. Figure 2B shows the mean Ca^{2+} increase observed after application of 0.1% DMSO alone (control), or various doses of CCH (1–20 μM) or 20 μM CCH plus the M1-selective antagonist pirenzepine (10 μM).[24,25] Lower doses of CCH (1 μM) did not significantly increase Ca^{2+} ($P > 0.05$; $n = 5$) compared with control. However, doses of 3 μM ($n = 11$) and 20 μM ($n = 12$) CCH produced significant increases in Ca^{2+} ($P < 0.01$) compared with control. The increase in Ca^{2+} seen with 20 μM CCH was reduced by more than 94% by 10 μM pirenzepine ($P < 0.0001$; $n = 11$). RT-PCR using primers specific for murine muscarinic receptor subtypes M1 to M5[23] revealed PCR amplification products for M1 and M4 receptors in Müller cells (Fig. 2C), whereas all muscarinic receptor subtypes were present in mouse retina (Fig. 2D). In addition to the predom-

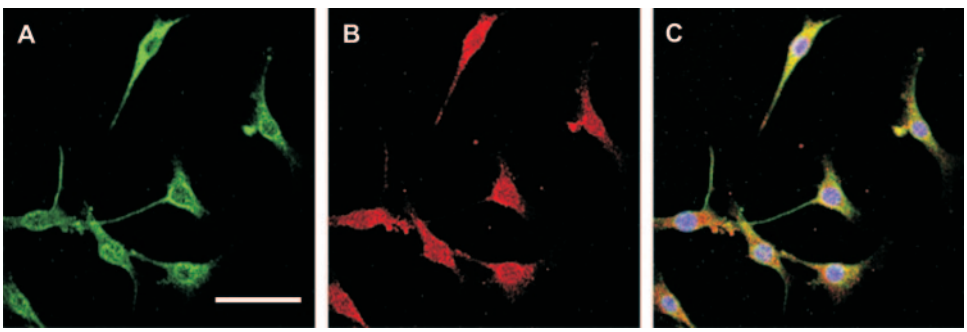

Figure 1. Immunocytochemical analysis of mouse Müller cells in primary culture. The purity of the Müller cell culture was tested by immunocytochemical analysis with Müller cell antigenic markers. Cells were seeded on glass coverslips for 1 to 2 days and probed with primary antibodies that label Müller cells. Immunostaining for (**A**) CRALBP and (**B**) GFAP. (**C**) Overlay image of CRALBP, GFAP, and TO-PRO 3, which was used to label the nuclei. Scale bar, 25 μM.

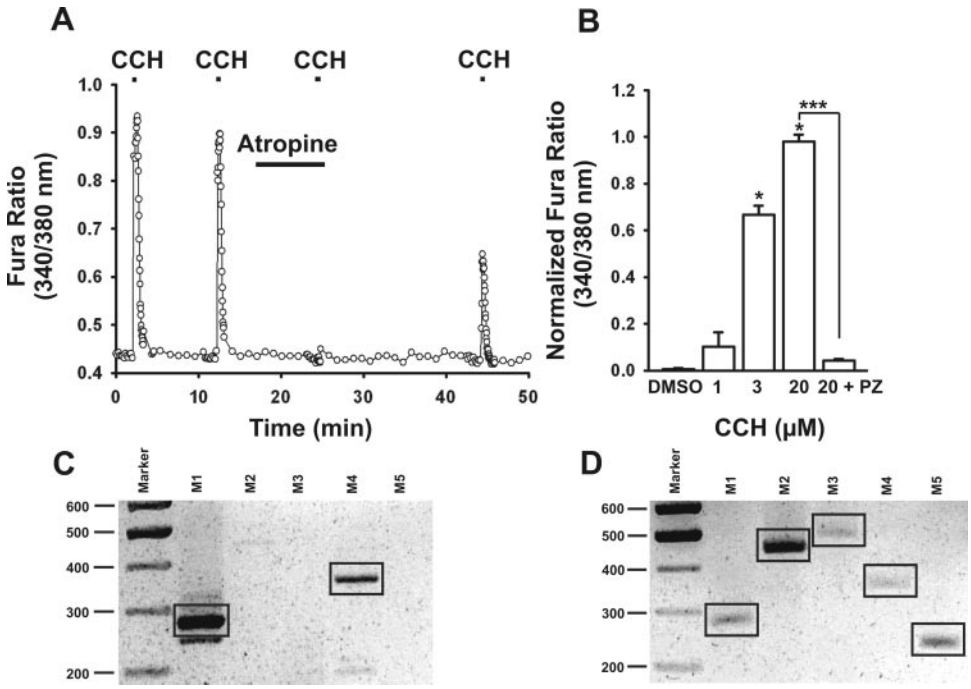

FIGURE 2. Activation of muscarinic receptors increases $[Ca^{2+}]_i$ in cultured Müller cells. (**A**) Repeated 30-second applications of 20 μM carbachol (CCH) induced increases in $[Ca^{2+}]_i$ that were blocked by 5 μM atropine. The CCH-induced $[Ca^{2+}]_i$ increase recovered partially after washing for 20 minutes ($n = 14$). (**B**) Histogram shows normalized mean ± SEM increases in $[Ca^{2+}]_i$ after cells were exposed for 45 to 60 seconds to DMSO vehicle ($n = 8$), 1 μM CCH ($n = 5$), 3 μM CCH ($n = 11$), 20 μM CCH ($n = 12$), and 20 μM CCH in the presence of 10 μM pirenzepine (PZ; $n = 11$), respectively. $^*P < 0.01$. $^{***}P < 0.0001$. (**C**, **D**) Total RNA from mouse Müller cells and whole retina was subjected to reverse transcriptase after DNase digestion and amplified with published sequences for muscarinic receptors. Amplified fragments were resolved by agarose-gel electrophoresis and visualized by ethidium bromide staining. M1 (273 bp), M2 (441 bp), M3 (511 bp), M4 (345 bp), and M5 (230 bp). Highlighted *box* indicates PCR product of appropriate size.

inant 273-bp amplicon present in retina and Müller cells, a less abundant PCR product of approximately 250 bp was also detected in cultured Müller cells that might have represented a splice variant, previously reported for the mouse M1 gene.[26] The presence of metabotropic M1 receptors in Müller is consistent with pirenzepine block of the CCH-activated Ca^{2+} increase.

The CCH-induced Ca^{2+} increase required release from intracellular stores. Figure 3A shows that after application of the irreversible SERCA pump inhibitor, thapsigargin (TG), which generates an increase in Ca^{2+} followed by depletion of intracellular Ca^{2+} stores, the response to CCH was completely eliminated. Figure 3B demonstrates the involvement of the PLC-dependent metabotropic receptor pathway in the CCH-induced Ca^{2+} increase. Application of the PLC blocker U73122 blocked the CCH-activated Ca^{2+} increase in the presence of intact intracellular Ca^{2+} stores. However, subsequent application of the reversible SERCA pump inhibitor cyclopiazonic acid (CPA) was still able to initiate Ca^{2+} release from stores to produce a sustained Ca^{2+} increase in the presence of U73122. The bar graph in Figure 3C shows the mean CCH-activated Ca^{2+} increase measured in the absence of drug (control; $n = 12$), in the presence of 10 μM of the L-type Ca^{2+} channel blocker nifedipine ($n = 9$), and of the TRP channel blockers La^{3+} ($n = 16$; 100 μM), 2-APB ($n = 3$; 100 μM), Gd^{3+} ($n = 16$; 100 μM), ruthenium red ($n = 9$; 20 μM), and flufenamic acid ($n = 8$; 100 μM). The CCH-activated Ca^{2+} increase was not significantly affected by block of L-type voltage-dependent Ca^{2+} channels or ruthenium red, but it was reduced by La^{3+} ($P < 0.01$), 2-APB ($P < 0.01$), Gd^{3+} ($P < 0.01$), and flufenamic acid ($P < 0.01$). The bar graph in Figure 3D shows the mean Ca^{2+} increase in response to 50 μM of the DAG derivative 1-oleyl-2-acetyl-sn-glycerol (OAG), which has been shown to directly activate some TRPC channels, including TRPC3 and TRPC6,[27,28] applied alone or coapplied with 1 μM CCH. The mean response in the absence of drug (0.1% DMSO control; $n = 8$) and to 1 μM CCH in the absence of OAG is also shown. OAG was able to increase Müller cell Ca^{2+} compared with control ($P < 0.0001$) when applied alone. Furthermore, coapplication of OAG with CCH produced an increase in Ca^{2+} that was greater than that seen with 1 μM CCH alone ($P < 0.001$). This suggests that DAG analogues, acting through non–store-dependent mechanisms, together with agonist-activated IP3-dependent release from intracellular Ca^{2+} stores, can give rise to enhanced Ca^{2+} entry.

The Role of Muscarinic Receptor Activation in Ca^{2+} Release from TG-Sensitive Ca^{2+} Stores and Store-Operated Ca^{2+} Entry

Both TG and CCH are able to generate capacitative Ca^{2+} entry in Müller cells. Figure 4A shows that the incubation of Müller cells in Ca^{2+}-free, followed by Ca^{2+}-containing, extracellular solution does not induce Ca^{2+} influx. However, the application of TG in Ca^{2+}-free extracellular solution results in an initial TG-induced Ca^{2+} release followed by store-operated Ca^{2+} entry when cells are reexposed to Ca^{2+}-containing extracellular solution (Fig. 4B). When CCH was applied in Ca^{2+}-free extracellular solution before the application of TG, the subsequent TG-induced Ca^{2+} increase was decreased, indicating that CCH and TG released Ca^{2+} from common intracellular stores (Fig. 4C). Figure 4D shows that repeated applications of CCH (5 minutes) in Ca^{2+}-free extracellular solution also produced increases in Ca^{2+} that were followed by capacitative Ca^{2+} entry, albeit smaller than those seen after the irreversible SERC inhibitor, TG, on the reintroduction of Ca^{2+}-containing extracellular solution.

Nonselective TRP-like Cation Channels and Store-Operated Ca^{2+} Entry

The bar graph in Figure 5A shows the mean TG-induced Ca^{2+} influx in the absence (0.1% DMSO control; $n = 17$) and presence of various drugs, including the L-type Ca channel blocker nifedipine ($n = 12$; 10 μM) and the TRP channel blockers[29] La^{3+}($n = 10$; 100 μM), 2-APB ($n = 5$; 100 μM), Gd^{3+} ($n = 26$; 100 μM), flufenamic acid ($n = 22$; 100 μM), and ruthenium red ($n = 6$; 20 μM). Pharmacologic properties of the TG-induced Ca^{2+} influx were similar to those of the CCH-activated Ca^{2+} increase in that nifedipine and ruthenium red did not significantly affect the Ca^{2+} increase, but La^{3+}, 2-APB, Gd^{3+}, and flufenamic acid inhibited the TG-induced Ca^{2+} influx ($P <$

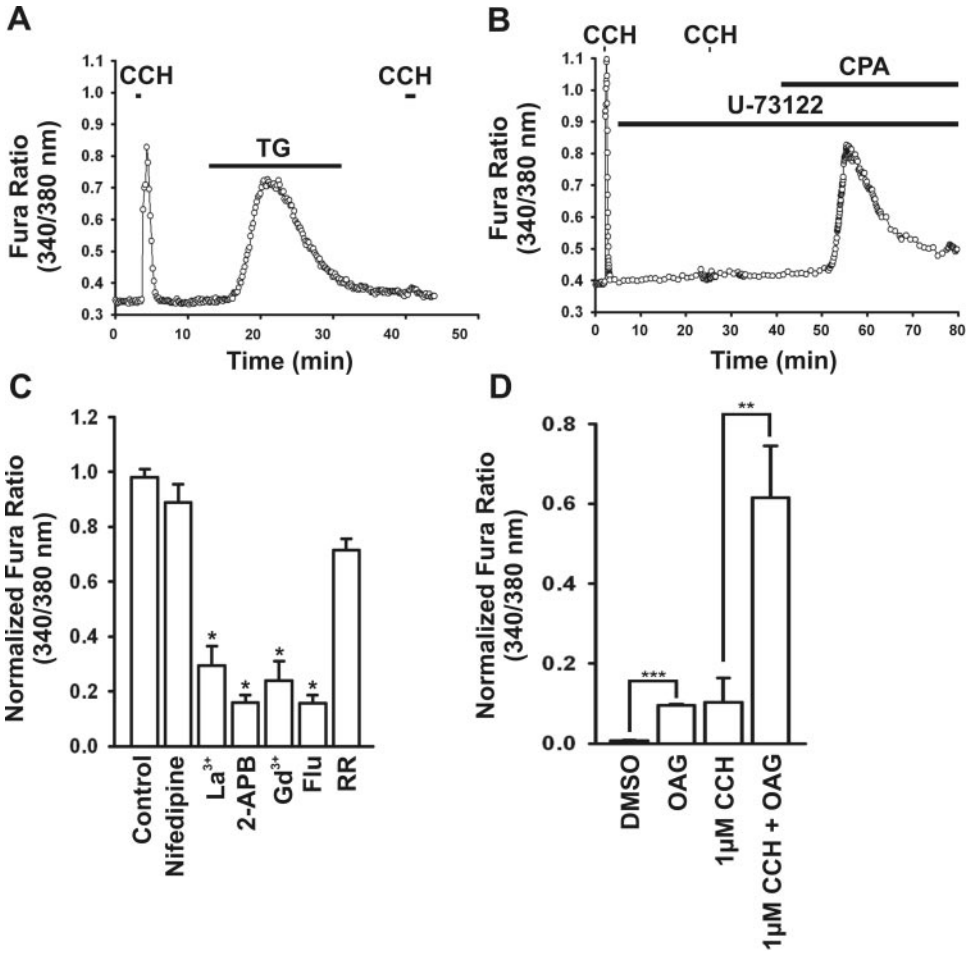

FIGURE 3. Ca^{2+} store depletion and block of PLC abolish CCH-activated $[Ca^{2+}]_i$ increases. (**A**) 20 μM CCH applied for 80 seconds produced a $[Ca^{2+}]_i$ increase. 40 nM thapsigargin induced a prolonged $[Ca^{2+}]_i$ increase, after which the CCH-induced $[Ca^{2+}]_i$ increase was abolished (n = 5). (**B**) Block of PLC with 5 μM U-73122 abolished the CCH-induced $[Ca^{2+}]_i$ increase; however, 5 μM CPA still induced a $[Ca^{2+}]_i$ increase (n = 10). (**C**) Histogram shows normalized mean ± SEM increases in fura-2 fluorescence ratio after Müller cells were exposed to CCH in the presence of 10 μM nifedipine (n = 9) and the following TRP channel blockers: 100 μM lanthanum chloride (La^{3+}; n = 16), 100 μM 2-aminoethoxydiphenly-borane (2-APB; n = 3), 100 μM gadolinium chloride (Gd^{3+}; n = 8), 100 μM flufenamic acid (Flu; n = 8), and 20 μM ruthenium red (RR; n = 9). Control (n = 12). $^*P < 0.01$. (**D**) Graph representing normalized mean ± SEM increases in fura-2 fluorescence in the presence of DMSO vehicle (n = 8), 50 μM OAG (n = 10), 1 μM CCH (n = 5), 1 μM CCH + 50 μM OAG (n = 5). $^{**}P < 0.001$. $^{***}P < 0.0001$.

0.01). The bar graph in Figure 5B shows the mean capacitative divalent influx after TG treatment in Ca^{2+}-free extracellular solution after the reintroduction of Ca^{2+} or of the Ca^{2+} substitutes Ba^{2+} and Sr^{2+}. Reintroduction of each of these ions produced a significant increase in the fura-2 ratio compared with divalent-free extracellular solution, suggesting that nonselective TRP-like cation channels may contribute to store-operated Ca^{2+} entry in Müller cells. Figure 6A shows RT-PCR analysis of TRPC channels using cDNA from mouse retina and purified Müller cell cultures, with primers specific for murine TRPC1–7 (Table 1). PCR products of the expected size for all TRPC channels, with the exception of TRPC2 (data not shown), were amplified from whole retina. In contrast, only the PCR product for TRPC1 and TRPC6 was amplified from cultured Müller cells. Further confirmation of the presence of TRPC1 and TRPC6 protein in Müller cells was carried out using immunocytochemical staining with antibodies specific to TRPC1 and TRPC6 protein. The TRPC1 antibody recognizes an epitope corresponding to amino residues 557 to 571 of human TRPC1, and the TRPC6 antibody is directed at residues 24 to 38 of murine TRPC6. Both antibodies have been demonstrated to detect TRPC1 and TRPC6 protein in expression systems,[30,31] in rodent and mouse brain[32,33] and retina,[34] and in cultured and isolated mouse astrocytes.[11,35] Consistent with the presence of mRNA for TRPC1 and TRPC6 in mouse Müller cells, immunofluorescence labeling for TRPC1 and TRPC6 protein was detected in cultured Müller cells (Fig. 6B, left panels) compared with the control preabsorbed antibody (Fig. 6B, right panels).

Patch-clamp recordings were carried out using K^+-free extracellular solution containing 100 μM $BaCl_2$ and CsCl pipette solutions to block K^+ channels. Figure 7A shows whole-cell current recorded at −120 mV and +80 mV in a representative Müller cell. Application of 20 μM CCH produced a reversible increase in whole-cell conductance. Figure 7B shows the current-voltage (I-V) relationship for current measured in the absence (a) and presence (b) of CCH for the cell shown in Figure 7A. Cells were held at −60 mV and stepped in 40-mV increments from −120 mV to +80 mV. The CCH-activated current exhibits weak outward rectification and reverses close to 0 mV (−0.19 ± 0.89 mV; n = 4), as would be expected for a nonselective cation current. The mean CCH-activated current measured in 10 cells at −120 mV and +80 mV was −5.85 ± 1.87 pA/pF and 4.88 ± 1.18 pA/pF, respectively. Figure 6C shows current recordings made at −120 mV and +80 mV before and after application of CCH plus 100 μM Gd^{3+} in a representative cell. Figure 7D shows the I-V for the peak current measured at 40 mV increments from −120 mV to +80 mV in the absence (a) and presence (b) of CCH plus Gd^{3+} for the cell shown in Figure 7C. The mean CCH-activated current (n = 3) in the presence of Gd^{3+} at −120 mV and +80 mV was −0.5 ± 0.12 pA/pF and 0.22 ± 0.55 pA/pF, respectively, and was reduced (>85%) compared with the control CCH-activated current ($P < 0.005$ at −120 mV).

DISCUSSION

This study provides novel data identifying essential components of the signaling pathway responsible for muscarinic agonist-mediated Ca^{2+} influx in mouse Müller cells. This signaling pathway is initiated by metabotropic muscarinic receptor activation, followed by subsequent activation of PLC, Ca^{2+}

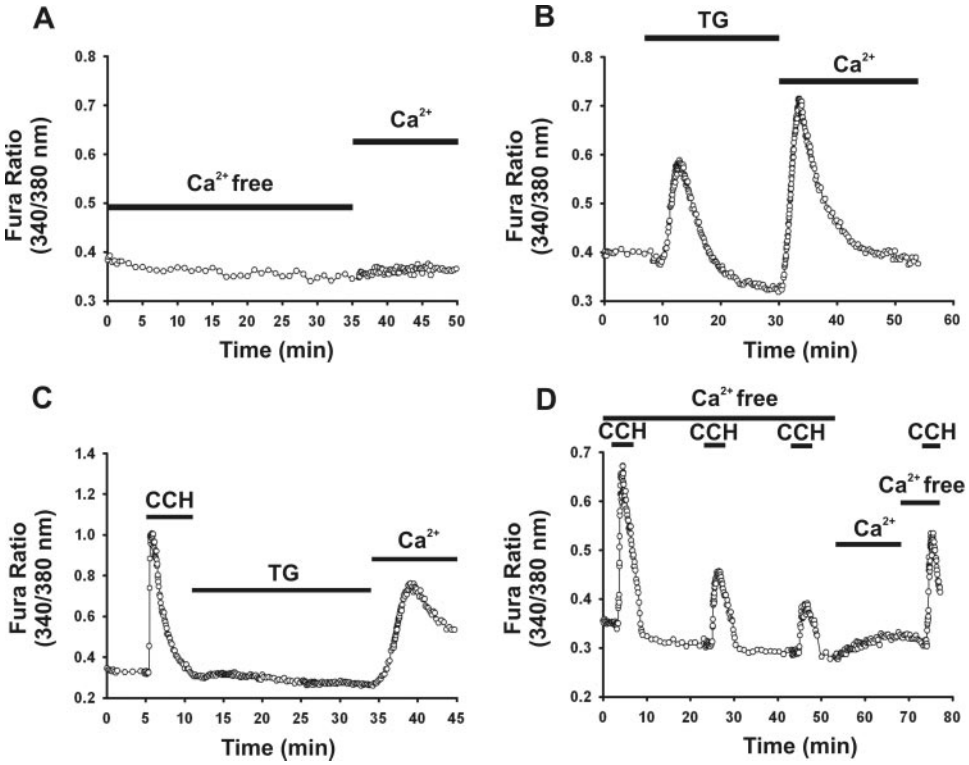

FIGURE 4. Depletion of intracellular Ca^{2+} stores activates store-operated Ca^{2+} entry. (**A**) Müller cells ($n = 11$) were incubated in Ca^{2+}-free followed by Ca^{2+}-containing extracellular solution, where no Ca^{2+} influx was observed. (**B**) 40 nM TG was applied to cells ($n = 17$) in Ca^{2+}-free extracellular solution to deplete intracellular Ca^{2+} stores. On return of $[Ca^{2+}]_i$ to baseline levels, 1 mM Ca^{2+} was added to the extracellular solution, resulting in store-operated Ca^{2+} entry and increase in fura-2 fluorescence ratio. (**C**) Exposure of Müller cells to 20 μM CCH in Ca^{2+}-free solution (5 minutes) decreased the subsequent TG-induced release of Ca^{2+} from intracellular Ca^{2+} stores. After this, 1 mM Ca^{2+} was added to the extracellular solution, resulting in store-operated Ca^{2+} influx and an increase in fura-2 fluorescence ($n = 5$). (**D**) Intracellular Ca^{2+} stores were depleted by repeatedly exposing cells for 5 minutes to 20 μM CCH in Ca^{2+}-free extracellular solution. On return of $[Ca^{2+}]_i$ to baseline, 1 mM Ca^{2+} was added to the extracellular solution, and this resulted in an increase in fura-2 fluorescence ratio, indicating a store-operated Ca^{2+} influx and a refilling of intracellular stores. Subsequently, cells were incubated in Ca^{2+}-free extracellular solution followed by 5-minute exposure to CCH, which resulted in a fluorescence increase, indicating the release of Ca^{2+} from intracellular stores ($n = 13$).

release from TG and CPA-sensitive Ca^{2+} stores, and Ca^{2+} influx through TRP-like nonselective cation channels, which may include TRPC1 and TRPC6.

In contrast to mouse retina, which expresses all five muscarinic receptor subtypes (M1-M5), only the PCR product for M1 and M4 receptors was amplified from cultured mouse Müller cells. Although M4 receptors preferentially coupled through Gi/o to adenyl cyclase, M1 receptors are coupled to metabotropic $G_{q/11}$-coupled receptors, activation of which is associated with PLC-dependent release of Ca^{2+} from IP_3-sensitive intracellular stores.[24,25] Consistent with the activation of M1 receptors in Müller cells, the M1-specific antagonist pirenzepine and the nonselective muscarinic receptor agonist atropine blocked CCH-activated Ca^{2+} increases. Our findings indicating that CCH activates metabotropic M1 receptors to mediate Ca^{2+} increases in mouse Müller cells are also supported by previous studies demonstrating that the M1 receptor-specific agonist McN-A-343 can increase Ca^{2+} in cultured rat and rabbit Müller cells.[21]

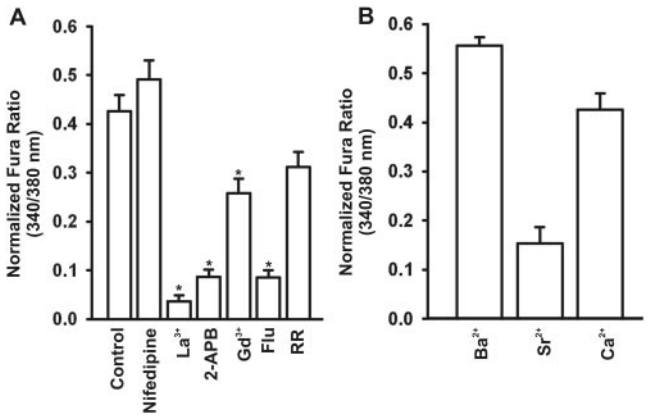

FIGURE 5. Intracellular Ca^{2+} store depletion induces influx of divalent cations. (**A**) 40 nM TG was applied to cells to deplete intracellular Ca^{2+} stores in Ca^{2+}-free extracellular solution. On return of $[Ca^{2+}]_i$ to baseline, 1 mM Ca^{2+} was added to the extracellular solution in the presence of 10 μM nifedipine ($n = 12$), 100 μM La^{3+} ($n = 10$), 100 μM 2-APB ($n = 5$), 100 μM Gd^{3+} ($n = 26$), 100 μM flufenamic acid (Flu; $n = 22$), and 20 μM ruthenium red (RR; $n = 6$). Control ($n = 17$). $^*P < 0.01$. (**B**) Müller cells were exposed to 40 nM TG in Ca^{2+}-free extracellular solution to deplete intracellular Ca^{2+} stores. When $[Ca^{2+}]_i$ reached baseline, 1 mM Ba^{2+}, 1 mM Sr^{2+}, or 1 mM Ca^{2+} was added to the extracellular solution, which resulted in increases in fura-2 fluorescence. The histogram indicates normalized mean ± SEM increases in fura-2 fluorescence after the addition of 1 mM Ba^{2+} ($n = 6$), Sr^{2+} ($n = 5$), or Ca^{2+} ($n = 17$) to Ca^{2+}-free extracellular solution.

We demonstrated that intracellular Ca^{2+} stores released by the activation of muscarinic receptors in Müller cells were common to those released by TG and that both muscarinic receptor activation and TG produced divalent influx. The pharmacology of the TG-mediated store-operated Ca^{2+} influx was similar to that of the CCH-activated Ca^{2+} increase, including

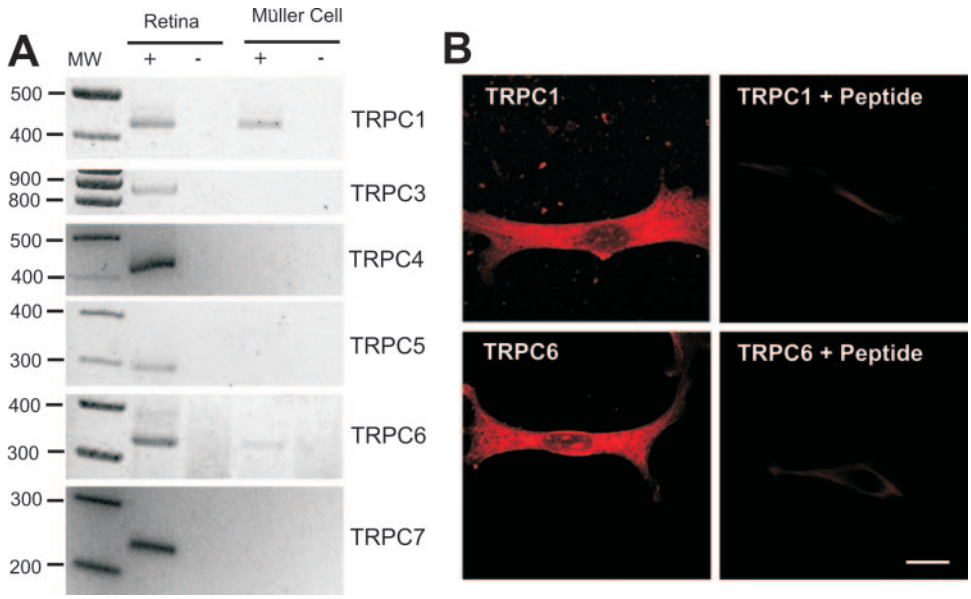

FIGURE 6. TRPC mRNA and protein in mouse Müller cells. mRNA from mouse retina or Müller cells was amplified with primers specific for TRPC1–7 (see Table 1). Amplified fragments were subjected to electrophoresis on agarose gel and visualized by ethidium bromide. (**A**) Representative gel showing amplification products for TRPC1 (427 bp), TRPC3 (831 bp), TRPC4 (414 bp), TRPC5 (287 bp), TRPC6 (332 bp), and TRPC7 (240 bp) in mouse retina and cultured mouse Müller cells. 100-bp ladder as molecular marker. (**B**) Immunocytochemical staining for TRPC1 (*upper left*) and TRPC6 protein (*lower left*) in Müller cells. *Right*: control staining (TRPC1, *upper*; TRPC6, *lower*) using primary antibody preabsorbed with antigen peptide. Scale bar, 15 μM.

block by the trivalent cations La^{3+} and Gd^{3+} and by 2-APB and flufenamic acid, providing support for TRP channel contributions in this pathway. Of the candidate TRP channels mediating Ca^{2+} entry induced by phospholipid hydrolysis and Ca^{2+} store depletion,[27–29] we suggest that the TRPC1 and TRPC6 isoforms, shown here to be present in Müller cells, may contribute to agonist-mediated divalent influx. In support of this are reports that both these TRP channels mediate receptor- and store-operated Ca^{2+} influx in a variety of cells.[10,11,15,27,30,34–36] Although the role of TRPC1 in store-operated Ca^{2+} influx is more established,[37] muscarinic receptor activation and TG-induced depletion of intracellular Ca^{2+} stores has been shown to increase TRPC6 exocytotic insertion into the plasma membrane in transfected HEK293 cells, suggesting that in some cells, IP_3-dependent Ca^{2+} mobilization from intracellular stores may be required for surface expression and subsequent activation of this channel.[38] Additionally, interaction between agonist-generated DAG and IP_3 was demonstrated to provide synergistic activation of TRPC6-like cation channels in rabbit portal vein smooth muscle cells.[39]

TRP channel expression and function have not been extensively studied in vertebrate retina, but several reports have now identified putative roles for TRPC channels. In chicken retina, immunoreactivity for TRPC1 and TRPC4 was identified, with TRPC1 staining localized to the inner plexiform layer and TRPC4 labeling more extensively distributed to all layers of the retina, including Müller cells.[40] Examination of Ca^{2+} entry pathways in mouse retina suggested that TRPC6 may operate as a putative store-operated Ca^{2+} channel in the cell body of rods, and TRPC6 immunoreactivity was also observed in the

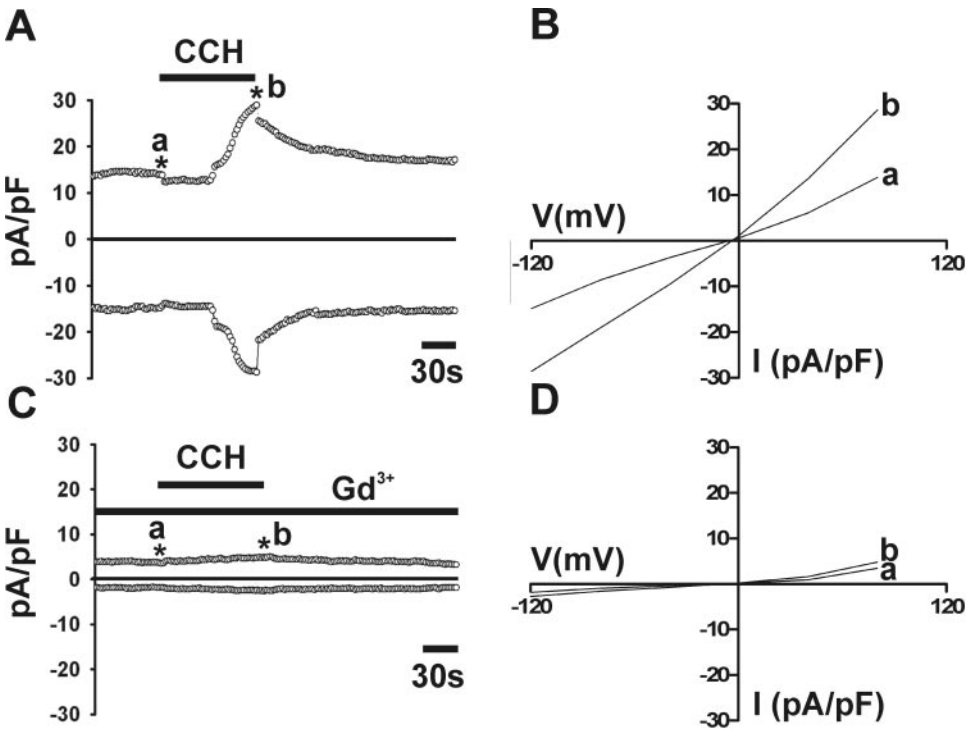

FIGURE 7. CCH activates a nonselective cation current. Whole-cell patch-clamp recordings were made from Müller cells (V_{hold} = −60 mV) in K^+-free solution (+100 μM $BaCl_2$). (**A**) Current measured at −120 mV and +80 mV before and after application of 20 μM CCH in a representative Müller cell. (**B**) I-V relationship for current measured in the absence (a) and presence (b) of CCH for the cell shown in (**A**). (**C**) Current measured in a representative cell at −120 mV and +80 mV before and after application of 10 μM CCH in the presence of 100 μM Gd^{3+}. (**D**) I-V relationship for peak current measured in the absence (a) and presence (b) of CCH plus Gd^{3+} for the cell shown in (**C**). For I-Vs shown in (**B**, **D**), current was sampled in 40-mV increments from −120 mV to +80 mV. Capacitance values for the cells shown are 56 pF for the cell in (**A**, **B**) and 37 pF for the cell shown in (**C**, **D**).

cell bodies of bipolar, amacrine, and retinal ganglion cells.[34] More recently, study[41,42] of the light-activated signaling pathway in rat suprachiasmatic nuclei-projecting retinal ganglion cells has provided additional evidence supporting the involvement of a G-protein–mediated signaling pathway and activation of a TRP-like cation current. The activity of this channel was enhanced by OAG, though OAG did not directly activate the channel, and was blocked by lanthanides and flufenamate. Consistent with this, immunohistochemical experiments identified labeling for TRPC6 in melanopsin-positive retinal ganglion cells and most other cells in the retina.[41] Our data are supportive of a contribution from OAG-sensitive TRPC channels, possibly TRPC6, to Ca^{2+} entry in mouse Müller cells; however, it is also possible that store-operated Ca^{2+} entry in these cells involves additional Ca^{2+} entry pathways because OAG and CCH produced enhanced Ca^{2+} entry when coapplied.

In the retina, Müller cells respond to the release of neuronal transmitters with increases in Ca^{2+} and have been shown to release glial factors to regulate neuronal activity and to modify arteriole diameters.[1,43] Ca^{2+} transients also occur spontaneously in Müller cells in the absence of neuronal activity, and their frequency is increased when the retina is illuminated.[43] In isolated retina, light-evoked Ca^{2+} increases in Müller cells are tetrodotoxin sensitive, suggesting that action potential–producing retinal neurons, possibly amacrine or ganglion cells, participate in neuron-to-glia signaling. Although light-evoked Ca^{2+} transients in Müller cells are predominantly mediated by the neuronal release of ATP,[44] it is possible that under appropriate illumination protocols, acetylcholine released from starburst amacrine cells[45,46] could facilitate Ca^{2+} signals in retinal glia. Furthermore, muscarinic receptor-mediated signaling in Müller cells may be more pronounced in retinal abnormalities in which phenotypic changes occurring in proliferative Müller cells could lead to alterations in receptor expression and metabotropic receptor-mediated Ca^{2+} signaling.[17,19] These changes may be recapitulated in Müller cells growing in culture.

References

1. Metea MR, Newman EA. Calcium signaling in specialized glial cells. *Glia*. 2006;54:650–665.
2. Scemes E, Giaume C. Astrocyte calcium waves: what they are and what they do. *Glia*. 2006;54:716–725.
3. Verkhratsky A. Glial calcium signaling in physiology and pathophysiology. *Acta Pharmacol Sin*. 2006;27:773–780.
4. Bird GS, Aziz O, Lievremont JP, et al. Mechanisms of phospholipase C-regulated calcium entry. *Curr Mol Med*. 2004;4:291–301.
5. Lewis RS. The molecular choreography of a store-operated calcium channel. *Nature*. 2007;446:284–287.
6. Parekh AB. On the activation mechanism of store-operated calcium channels. *Pflugers Arch*. 2006;453:303–311.
7. Putney JW Jr. Capacitative calcium entry: sensing the calcium stores. *J Cell Biol*. 2005;169:381–382.
8. Bergdahl A, Gomez MF, Wihlborg AK, et al. Plasticity of TRPC expression in arterial smooth muscle: correlation with store-operated Ca^{2+} entry. *Am J Physiol*. 2005;288:C872–C880.
9. Brueggemann LI, Markun DR, Henderson KK, Cribbs LL, Byron KL. Pharmacological and electrophysiological characterization of store-operated currents and capacitative Ca^{2+} entry in vascular smooth muscle cells. *J Pharmacol Exp Ther*. 2006;317:488–499.
10. Rao JN, Platoshyn O, Golovina VA, et al. TRPC1 functions as a store-operated Ca^{2+} channel in intestinal epithelial cells and regulates early mucosal restitution after wounding. *Am J Physiol*. 2006;290:G782–G792.
11. Golovina VA. Visualization of localized store-operated calcium entry in mouse astrocytes: close proximity to the endoplasmic reticulum. *J Physiol*. 2005;564:737–749.
12. Hayat S, Wiqley CB, Robbins J. Intracellular calcium handling in rat olfactory ensheathing cells and its role in axonal regeneration. *Mol Cell Neurosci*. 2003;22:259–70.
13. Kawasaki BT, Liao Y, Birnbaumer L. Role of Src in C3 transient receptor potential channel function and evidence for a heterogeneous makeup of receptor- and store-operated Ca^{2+} entry channels. *Proc Natl Acad Sci U S A*. 2006;103:335–340.
14. Cheng HW, James AF, Foster RR, Hancox JC, Bates DO. VEGF activates receptor-operated cation channels in human microvascular endothelial cells. *Arterioscler Thromb Vasc Biol*. 2006;26:1768–1776.
15. Soboloff J, Spassova M, Xu W, He LP, Cuesta N, Gill DL. Role of endogenous TRPC6 channels in Ca^{2+} signal generation in A7r5 smooth muscle cells. *J Biol Chem*. 2005;280:39786–39794.
16. Grimaldi M, Maratos M, Verma A. Transient receptor potential channel activation causes a novel form of [Ca^{2+}] oscillations and is not involved in capacitative Ca^{2+} entry in glial cells. *J Neurosci*. 2003;23:4737–4745.
17. Bringmann A, Pannicke T, Grosche J, et al. Müller cells in the healthy and diseased retina. *Prog Retinal Eye Res*. 2006;25:397–424.
18. Newman EA, Reichenbach A. The Müller cell: a functional element of the retina. *Trends Neurosci*. 1996;19:307–312.
19. Bringman A, Pannike T, Weick M, et al. Activation of P2Y receptors stimulates potassium and cation currents in acutely isolated human Muller (glial) cells. *Glia*. 2002;37:139–152.
20. Puro DG. Stretch-activated channels in human retinal Mueller cells. *Glia*. 1991;4:456–460.
21. Wakakura M, Utsunomiya-Kawasaki I, Ishikawa S. Rapid increase in cytosolic calcium ion concentration mediated by acetylcholine receptors in cultured retinal neurons and Muller cells. *Graefes Arch Clin Exp Ophthalmol*. 1998;236:934–939.
22. Wang Z, Li W, Mitchell CK, Carter-Dawson L. Activation of protein kinase C reduces GLAST in the plasma membrane of rat Müller cells in primary culture. *Vis Neurosci*. 2003;20:611–619.
23. Aihara T, Nakamura Y, Taketa MM, Matsui M, Okabe S. Cholinergically stimulated gastric acid secretion is mediated by M(3) and M(5) but not M(1) muscarinic acetylcholine receptors in mice. *Am J Physiol*. 2005;288:G1199–G1120.
24. Yang Q, Sumner AD, Puhl HL, Ruiz-Velasco V. M(1) and M(2) muscarinic acetylcholine receptor subtypes mediate Ca(2+) channel current inhibition in rat sympathetic stellate ganglion neurons. *J Neurophysiol*. 2006;96:2479–2487.
25. Caulfield MP, Birdsall NJ. International Union of Pharmacology, XVII: classification of muscarinic acetylcholine receptors. *Pharmacol Rev*. 1998;50:279–290.
26. Wood IC, Garriga Canut M, Palmer CL, Pepitoni S, Buckley NJ. Neuronal expression of the rat M1 muscarinic acetylcholine receptor gene is regulated by elements in the first element. *Biochem J*. 1999;340:475–483.
27. Thebault S, Zholos A, Enfissi A, et al. Receptor-operated Ca^{2+} entry mediated by TRPC3/TRPC6 proteins in rat prostate smooth muscle (PS1) cell line. *J Cell Physiol*. 2005;204:320–328.
28. Dietrich A, Gudermann T. TRPC6. *Handb Exp Pharmacol*. 2007;179:125–141.
29. Clapham DE, Montell C, Schultz G, Julius D. International Union of Pharmacology, XLIII: compendium of voltage-gated ion channels: transient receptor potential channels. *Pharmacol Rev*. 2003;55:591–596.
30. Liu X, Singh BB, Ambudkar IS. TRPC1 is required for functional store-operated Ca^{2+} channels. *J Biol Chem*. 2003;278:11337–11343.
31. Sours S, Du J, Chu S, Ding M, Zhou XJ, Ma R. Expression of canonical transient receptor potential (TRPC) proteins in human glomerular mesangial cells. *Am J Physiol Renal Physiol*. 2006;290:F1507–F1515.
32. Strubing C, Krapivinsky G, Krapinvinsky L, Clapham DE. Formation of novel TrpC channels by complex subunit interactions in embryonic brain. *J Biol Chem*. 2003;278:39014–39019.
33. von Bohlen und Halbach O, Hinz V, Unsicker K, Egorov A. Distribution of TRPC1 and TRPC5 in medial temporal lobe structures of mice. *Cell Tissue Res*. 2005;322:201–206.

34. Krizaj D. Compartmentalization of calcium entry pathways in mouse rods. *Eur J Neurosci*. 2005;22:3292–3296.
35. Beskina O, Miller A, Mazzocco-Spezzia A, Pulina MV, Golovina VA. Mechanisms of interleukin-1β-induced Ca^{2+} signals in mouse cortical astrocytes: roles of store- and receptor-operated Ca^{2+} entry. *Am J Physiol Cell Physiol*. 2007;293:C1103–C1111.
36. Jung S, Strotmann R, Schultz G, Plant TD. TRPC6 is a candidate channel involved in receptor-stimulated cation currents in A7r5 smooth muscle cells. *Am J Physiol Cell Physiol*. 2002;282:C347–C359.
37. Ambudkar IS. TRPC1: a core component of store-operated calcium channels. *Biochem Soc Trans*. 2007;35:96–100.
38. Cayouette S, Lussier MP, Mathieu EL, Bousquet SM, Boulay G. Exocytotic insertion of TRPC6 channel into the plasma membrane upon Gq protein-coupled receptor activation. *J Biol Chem*. 2004; 279:7241–7246.
39. Albert AP, Large WA. Synergism between inositol phosphates and diacylglycerol on native TRPC6-like channels in rabbit portal vein myocytes. *J Physiol*. 2003;552:789–795.
40. Crousillac S, LeRouge M, Rankin M, Gleason E. Immunolocalization of TRPC channel subunits 1 and 4 in the chicken retina. *Vis Neurosci*. 2003;20:453–463.
41. Warren EJ, Allen CN, Lane Brown R, Robinson DW. The light-activated signaling pathways in SCN-projecting rat retinal ganglion cells. *Eur J Neurosci*. 2006;23:2477–2487.
42. Sekeran S, Lall GS, Ralphs KL, et al. 2-Aminoethoxydiphenylborane is an acute inhibitor of direct photosensitive retinal ganglion cell activity *in vitro* and *in vivo*. *J Neurosci*. 2007;27:3981–3986.
43. Metea MR, Newman EA. Signaling within the neurovascular unit in the retina. *Exp Physiol*. 2007;92:635–640.
44. Newman EA. Calcium increases in retinal glial cells evoked by light-induced neuronal activity. *J Neurosci*. 2005;25:5502–5510.
45. Neal M, Cunningham J. Modulation by endogenous ATP of the light-evoked release of ACh from retinal cholinergic neurones. *Br J Pharmacol*. 1994;113:1085–1087.
46. Massey SC, Redburn DA. Light-evoked release of acetylcholine in response to a single flash: cholinergic amacrine cells receive ON and OFF input. *Brain Res*. 1985;328:374–377.